Theory of Hypervalency: Recoupled Pair Bonding in SF_n ($n = 1-6$)

David E. Woon* and Thom H. Dunning, Jr.*

Department of Chemistry, University of Illinois at Urbana–Champaign, Box 92-6, CLSL, 600 South Mathews, Urbana, Illinois 61801

Received: March 3, 2009; Revised Manuscript Received: April 30, 2009

To gain new insight into the nature of hypervalency, we have characterized the bonding across the entire SF_n sequence ($n = 1-6$) with high-level quantum chemical theory (multireference configuration interaction and coupled cluster calculations using correlation consistent basis sets). In contrast to most previous studies, this work examined both the stable equilibrium structures and the process of SF_n−F bond formation. We conclude that two different types of bonding can occur in these species: normal polar covalent bonding and a new type that we call recoupled pair bonding. The two bonding processes can be seen in diatomic SF, where hypervalent behavior first occurs. In the covalently bonded $^2\Pi$ ground state, the bond is formed by straightforward singlet coupling of electrons in the singly occupied S 3p and F 2p orbitals. But there is also a low-lying $^4\Sigma^-$ excited state where the S $3p^2$ pair of electrons must first be decoupled so that one of the electrons can singlet couple with the electron in the F 2p orbital, hence the term recoupled pair bonding. Energy is required to decouple the electron pair, but the bond energy of SF($^4\Sigma^-$) is still a substantial fraction (about 40%) of the bond energy of SF($^2\Pi$). Recoupled pair bonding is the basis for hypervalent behavior: for example, the three unpaired electrons of SF($^4\Sigma^-$) are available for further bond formation, and their spatial orientations clearly anticipate the structure of SF_4. The new model of hypervalent bonding introduced in this work accounts for the observed trends in the structures of SF_n molecules and the variations in the (SF_n−F) bond energies. The model also predicts the existence of low-lying excited states in some SF_n species and provides explanations for their energetic separations and orderings.

1. Introduction

Many general chemistry textbooks—and some from more advanced courses—continue to attribute the origin of hypervalency to Pauling[1] d-orbital hybridization. While most of the chemistry community has long recognized[2–5] that d-orbital hybridization is not an acceptable explanation for the origin of hypervalent behavior, we will show in the present study that the prevailing theoretical model, Rundle−Pimentel[6–8] three-center/four-electron (3c/4e) bonding, has overlooked fundamental aspects of the nature of hypervalency. We will describe a new model for hypervalency that we call *recoupled pair bonding*. Hypervalent bonding occurs when it is "energetically favorable"[9] to decouple a pair of electrons in order to form a new bond. Much of the insight gained by this model is the result of examining the process of bond formation rather than focusing only on stable species near their equilibrium geometries, as other models have done. Using the SF_n ($n = 1-6$) series, we will demonstrate that recoupled pair bonding is responsible for the origin of hypervalent behavior. The model provides ready explanations for the well-known oscillation of bond energies in the SF_n series and the lesser known presence of low-lying excited states in SF and SF_2, and it accounts straightforwardly for the structures of the SF_n species. In addition, this approach to characterizing hypervalency has identified a striking commonality between the bonding in some sulfur and carbon species.

In 1969, Musher[10] introduced the term *hypervalent* to describe the behavior of certain elements that are able to form more bonds than expected upon the basis of the predominant valence of the lightest element in the same group, while Schleyer[11] introduced the related term *hypercoordinate* in 1984. Phosphorus, sulfur, and chlorine are the archetypical hypervalent elements. Compounds such as PF_5, SF_6, and ClF_3 are experimentally stable, while the corresponding species NF_5, OF_6, and F_4 have not been observed. Hypervalency was extended to include the heavier rare gases[12] with the discovery of stable xenon fluoride species. However, Musher tracked down citations to hypercoordinated compounds that are now nearly two centuries old, dating back to Davy's report[13] of PCl_5 synthesis in 1810.

The notion that d-orbital hybridization is responsible for the origin of hypervalent behavior continued to be favored through the 1960s,[14] but a series of studies (mostly computational) demonstrated that a new model was needed (see Gilheany[3] for a detailed narrative). Jensen[15] briefly summarizes the work that led to the general acceptance of the Rundle−Pimentel 3c/4e bonding model. McGrady and Steed[16] provide an overview of the model, where p orbitals aligned with the axis defined by the hypervalent atom and two electronegative atoms or groups combine to form three-center bonding and antibonding MOs and a two-center nonbonding MO; the bonding and nonbonding orbitals are doubly occupied, while the antibonding orbital is unoccupied.

Our analysis of bonding in the SF_n family of molecules has led to new and unique insights that indicate that the 3c/4e model provides an incomplete description of hypervalency. Our model was derived by studying the ground and low-lying excited states of SF_n species through SF_6, the addition pathways ($SF_n + F \rightarrow SF_{n+1}$) that connect them, and the changes that occur in their orbitals during bond formation. Building molecules one atom at a time provides unrivaled insights into the nature of bonding and stands in contrast to models that focus on stable molecules

* To whom correspondence should be addressed. E-mail: dewoon@uiuc.edu (D.E.W.), tdunning@ncsa.uiuc.edu (T.H.D.).

10.1021/jp901949b CCC: $40.75
Published on Web 06/05/2009

and downplay the detailed pathways to their formation and the insight that intermediate species can provide. Likewise, there is also considerable insight to be gained by characterizing bond formation as a dynamic process where all of the valence electrons in the two reacting fragments shift in large or small ways to accommodate the formation of the new bond. In the case of hypervalent behavior, this atom-by-atom approach suggests that the key to understanding the nature of bonding in SF_4 and SF_6 is to first understand the bonding modes in SF, SF_2, SF_3, and SF_5. With a solid understanding of why hypervalent bonding is favorable in SF_n species, one can then explore other cases where it does not occur: an examination of the behavior of OF would provide insight into why S and O behave so differently, while HS would shed light on why SF_4 is stable but H_4S is not observed. Finally, an understanding of the basis for hypervalent behavior in these species might suggest parallels to bonding in other molecules not usually associated with hypervalency.

After briefly describing the methodology that we employed, the remainder of this paper will explore the nature of hypervalency in the SF_n family of molecules, from SF through SF_6, as well as SF^+ and SF^-. Our primary finding is that hypervalency arises from a *type of bond formation*. The new type of bond, which differs from normal covalent bonding, involves decoupling a pair of electrons, both of which can be recoupled with other electrons to form new chemical bonds. We thus identify this process as *recoupled pair bonding*. We find that even the simple diatomic SF has a low-lying state with a hypervalent bond, while SF_2 has two excited states with hypervalent bonds. Defining hypervalency as recoupled pair bonding supersedes previous notions that are limited to the properties of stable hypercoordinated molecules without full consideration of bond formation and intermediate species. The new understanding of hypervalency presented in this work provides a sound explanation for many properties of SF_n molecules, including their structures and spectra as well as the oscillations in the sequential SF_n−F bond energies that were observed nearly 30 years ago (see Figure 6 in Kiang and Zare[17]). As a consequence of identifying the source of hypervalent behavior, the new model has much improved predictive capability over prior models.

Another important consequence of this new perspective is that the bonding behavior in the SF_n family is found to strongly resemble the bonding that occurs in elements that are not traditionally considered to be hypervalent, in particular carbon. In section 6, we will show that the recoupling of valence ($3p^2$, $3s^2$) electrons in sulfur to form SF_n species is functionally equivalent to the recoupling of valence ($2s^2$) electrons in carbon to form the CH_n series, making recoupled pair bonding a very significant type of bonding, rather than an exception that occurs only in heavier chalcogen, pnictogen, halogen, or rare gas elements.

The study of SF_n species began with the synthesis of SF_6 by Moissan[18] in 1900, part of the body of work[19] that was recognized by the 1906 Nobel Prize in chemistry.[20] A thorough review of the experimental and theoretical literature on the structure, spectra, and properties of SF_n species is beyond the scope of this work, but we have attempted to compile a reasonably complete bibliography in the Supporting Information for this paper. Although it was carried out at a lower level of theory, the most thorough prior theoretical study of the low-lying states of SF_n species is the work of Ziegler and Gutsev.[21] Specific references to previous experimental and theoretical work will be described in context later in the paper.

2. Methodology

All calculations presented in this study were performed with the Molpro suite of quantum chemical programs (version 2002.6).[22] Multireference methods were used for calculations on SF and its ions and for treating bond formation in SF_3 and SF_5. Complete active space self-consistent field (CASSCF) calculations[23] provide the flexibility needed to account for the formation and dissociation of both covalent and hypervalent bonds. Degenerate occupations were averaged together in Π and Δ states. Internally contracted single and double excitation multireference configuration interaction (MRCI) calculations[24] were subsequently performed in some cases, including the Davidson correction[25] for quadruple excitations (designated as MRCI+Q). Structures and energies were also determined for minima and transition states of each neutral SF_n species with single-reference restricted singles and doubles coupled cluster theory[26] with perturbative triples [CCSD(T), RCCSD(T)].

Augmented correlation consistent basis sets (aug-cc-pVXZ) as large as quintuple ζ quality were used for F, and the corresponding d-function augmented sets [aug-cc-pV(X+d)Z] were used for S.[27] All of the stable SF_n species were treated at least at the RCCSD(T)/aug-cc-pVQZ level, which places the equilibrium bond dissociation energies and equilibrium structures reported in this work near state-of-the-art accuracy. The shorthand notation AV*X*Z (X = T, Q, 5) will be used to represent the sets of a specific quality. Extrapolations of total energies to estimated complete basis set (CBS) limits were performed where possible using the expression

$$E(x) = E_{\mathrm{CBS}} + b\mathrm{e}^{-x} + c\mathrm{e}^{-x^2} \quad (1)$$

where x is an integer corresponding to the basis set quality (DZ = 2, etc.) and E_{CBS}, b, and c are parameters derived from a least-squares fit to the calculated total energies.

For SF, spectroscopic parameters were determined via Dunham analysis[28] of potential energy curves derived from a least-squares fit to at least nine points around the minima. Dissociation energies (D_e) at the MRCI or MRCI+Q levels were computed by moving the fragments to a separation of at least 100 Å and subtracting the energy at r_e, while those at the RCCSD(T) level were computed from the energies of the isolated fragments. For SF, computed values of ω_e were used to correct the calculated values of D_e for vibrational zero-point energy (ZPE) to yield D_0 bond dissociation energies. For the ground states of SF_2−SF_6, we applied the reported ZPE corrections of Bauschlicher and Ricca[29] (see their Table 2). Dipole moments (μ_e) were computed at the MRCI level as expectation values or at the RCCSD(T) level via finite field calculations using an applied field of ±0.001 au (values are insensitive beyond 0.001 D for field strengths from 0.0005 to 0.005 au).

Bonding in the SF_n species will be described using natural orbitals (NOs) obtained from CASSCF calculations and approximate GVB orbitals[30] that were obtained by transforming the NOs using the CI coefficients for the relevant configurations

$$\sigma_R = \sqrt{\frac{c'_1}{c'_1 - c'_2}}\sigma_b + \sqrt{\frac{-c'_2}{c'_1 - c'_2}}\sigma_a$$
$$\sigma_L = \sqrt{\frac{c'_1}{c'_1 - c'_2}}\sigma_b - \sqrt{\frac{-c'_2}{c'_1 - c'_2}}\sigma_a \quad (2)$$

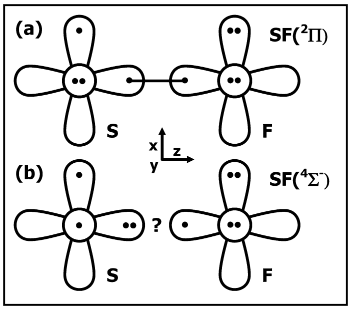

Figure 1. Atomic orbital configurations that give rise to low-lying molecular states of SF: (a) SF($^2\Pi$) and (b) SF($^4\Sigma^-$).

where σ_R and σ_L are the approximate GVB orbitals, σ_b and σ_a are the bonding and antibonding NOs, respectively, and c'_1 and c'_2 are renormalized CI vector coefficients from the CASSCF calculations. The overlap (S_{RL}) of the approximate GVB orbitals is given by

$$S_{RL} = \frac{c'_1 + c'_2}{c'_1 - c'_2} \qquad (3)$$

Contour (2D) and isodensity (3D) plots of orbitals were generated with gnuplot (http://www.gnuplot.info) and gOpenMol (http://www.csc.fi/gopenmol), respectively.

In addition to the static figures presented and discussed below, we have also generated a variety of animations, which are provided as Supporting Information. We will refer to these figures as S01, S02, and so on. The Supporting Information also includes an introductory discussion that compares the CASSCF and GVB orbital treatments of bond formation.

3. Covalent and Hypervalent States of SF

3.1. Bonding in the $^2\Pi$ and $^4\Sigma^-$ States of SF. Sulfur monofluoride possesses two low-lying states that serve as exemplars of covalent and recoupled pair (hypervalent) bonding, and we will compare and contrast their behavior in some detail. While Yang and Boggs[31] recently reported a very thorough treatment of all 12 valence states of SF that can be formed from ground state atoms, we are examining the nature of bonding in much greater depth for the two states of interest. Only one other previous theoretical study[32] examined the $^4\Sigma^-$ state, but neither paper considered the implications of its stability for our understanding of hypervalent bonding. To the best of our knowledge, the $^4\Sigma^-$ state of SF has not been observed or characterized in the laboratory.

As shown in Figure 1a, the $^2\Pi$ ground state of SF is formed straightforwardly when ground state S(^{3}P) and F(^{2}P) atoms approach with their singly occupied valence orbitals aligned along the internuclear axis. A traditional covalent electron pair bond is formed if the electrons in the S 3p$_z$ and F 2p$_z$ orbitals are coupled together as a singlet pair. The other three S valence 3p electrons are distributed in π_x and π_y orbitals (one of the two degenerate configurations is shown in the figure). An alternative approach of the two atoms is depicted in the Figure 1b, where the S atom is now rotated so that the doubly occupied 3p orbital lies along the internuclear axis and both singly occupied S 3p orbitals are off-axis. With the singly occupied F 2p$_z$ orbital on-axis, this yields a molecular state of $^4\Sigma^-$ symmetry if the three unpaired electrons have parallel spins. Interactions of this type, between a pair of electrons in an orbital on one atom and an unpaired electron in an orbital on another atom,

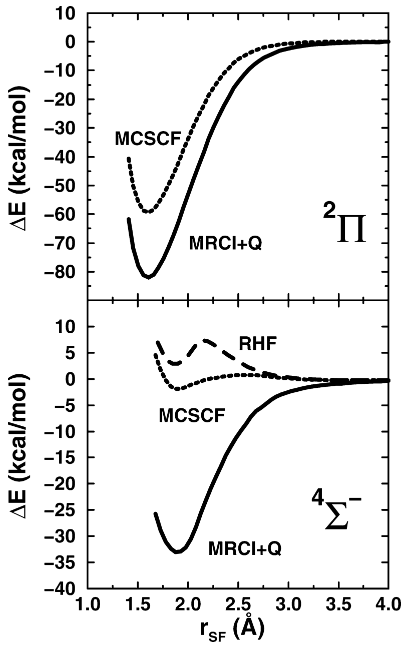

Figure 2. Potential energy curves of the low-lying $^2\Pi$ and $^4\Sigma^-$ states of SF at various levels of theory with AV5Z basis sets.

are often found to be repulsive [for example, NeF($^2\Sigma^+$), HF($^3\Pi$), and HS($^4\Sigma^-$)]. However, calculations show that SF($^4\Sigma^-$) is in fact decidedly bound at fully correlated levels of theory, as shown in Figure 2, which compares potential energy curves for the lowest-lying $^2\Pi$ and $^4\Sigma^-$ states of SF computed at several levels of theory. In addition to being bound by over 30 kcal/mol, there is not even a barrier to hinder the formation of SF($^4\Sigma^-$) when dynamic correlation is included (although there are modest barriers at the CASSCF and RHF levels of theory).

The bond energy of SF($^4\Sigma^-$) is about 40% of the bond energy of the $^2\Pi$ ground state. At the MRCI+Q/CBS level of theory, the dissociation energies (D_e) of the two states are 82.3 and 33.1 kcal/mol. With ω_e values of 840.9 and 513.8 cm^{-1} computed at the MRCI+Q/AV5Z level for the $^2\Pi$ and $^4\Sigma^-$ states, respectively, the respective values of D_0 are 81.1 and 32.4 kcal/mol. Analogous predictions at the RCCSD(T) level yield slightly larger D_0 values of 83.4 and 35.8 kcal/mol (from estimated CBS D_e values of 84.6 and 36.6 and corresponding AV5Z ω_e values of 842.8 and 504.7 cm^{-1}). The MRCI+Q prediction for the ground state is very close to two of the three experimental D_0 values, which include studies by Kiang and Zare (81.2 ± 1.6),[17] Hildenbrand (81.0 ± 1.2),[33] and Fisher et al. (77.5 ± 4.2).[34] The RCCSD(T) value is very similar to other calculations at high levels of theory[29,35–38] (see Table 1). No experimental value of ω_e has been reported to date for the ground state measured in either the gas phase or a cryogenic matrix, but Hassanzadeh and Andrews[39] attributed peaks observed at 822.1 and 818.8 cm^{-1} in Ar matrix studies to SF($^2\Pi$) (anharmonic frequencies ν).

The computed equilibrium bond length (r_e) is much larger for the excited state, 1.605 vs 1.901 Å, for the $^2\Pi$ and $^4\Sigma^-$ states, respectively, at the MRCI+Q/AV5Z level and 1.598 and 1.878 Å at the RCCSD(T)/AV5Z level. Experimental values for the bond length of the ground state include measurements by Carrington et al.[40] (r_0 = 1.599 ± 0.002 Å), Amano and Hirota[41] (r_e = 1.601 Å), and Endo et al.[42] (r_0 = 1.55946 Å). The observed dipole moment (μ_0) of the $^2\Pi$ ground state reported by Byfleet et al.[43] is 0.87 ± 0.05 D; the respective computed values (μ_e)

TABLE 1: A Comparison between Prior High Level Calculated Values of Ground State SF_n Bond Dissociation Energies and This Work

bond[a]	this work	ref 35[e]	ref 36[f]	ref 29[g]	ref 37[h]	ref 38[i]
$SF \rightarrow S + F$	81.1[b] 83.4[c]	81.8	82.4	82.8	83.0	83.2
$SF_2 \rightarrow SF + F$	89.5[d]	88.7	89.3	89.1	88.6	89.1
$SF_3 \rightarrow SF_2 + F$	54.5[d]	54.4	54.2	53.1	54.2	54.8
$SF_4 \rightarrow SF_3 + F$	96.2[d]	95.5	95.2	95.8	94.5	95.5
$SF_5 \rightarrow SF_4 + F$	39.2[d]	38.1	37.9	36.6	39.0	37.7
$SF_6 \rightarrow SF_5 + F$	105.6[d]	106.9	106.0	106.8	105.6	104.8

[a] Energies are in kcal/mol; all results are D_0 values, unless otherwise noted. [b] MRCI+Q level at estimated complete basis set (CBS) level (AVTZ, AVQZ, AV5Z). [c] RCCSD(T)/CBS. [d] RCCSD(T)/AVQZ results. [e] G2 or G2(MP2) results. [f] G2′/G2-(MP2) results. [g] CCSD(T)/CBS results (DZ, TZ, QZ). [h] G3 results (D_{298}). [i] DTQ results.

for the $^2\Pi$ and $^4\Sigma^-$ states are 0.786 and 2.577 D at the MRCI/AV5Z level and 0.789 and 2.600 D at the RCCSD(T)/AV5Z level.

To make sense of the surprising stability of SF($^4\Sigma^-$) and the relationship between the bond energies and bond lengths of this state and the ground state, we will examine the orbitals that are most critical to bond formation as the separated atoms come together to form the two states of the diatomic molecule. The natural and GVB bonding orbitals for the $^2\Pi$ and $^4\Sigma^-$ states at representative separations are shown together in Figure 3 (for animations and additional details about the bonding in both states, see S01−S06 in the Supporting Information).

The bonding orbitals in the $^2\Pi$ ground state (Figure 3a) are typical of polar covalent (moderately ionic) bonding orbitals. In the natural orbital model, the doubly occupied σ bonding orbital that forms from the singly occupied S and F atomic orbitals is concentrated on F at r_e. The σ antibonding orbital [which is only weakly occupied (0.04) at r_e] is delocalized but retains much of the original S character. In the GVB model, the $7\sigma_R$ orbital, which correlates with the F $2p_z$ orbital in the dissociated limit, is nearly unchanged at all separations, shifting very slightly toward S as the internuclear separation decreases. While this is happening, the $7\sigma_L$ orbital (the S $3p_z$ orbital at $r_{SF} = \infty$) delocalizes to the point where it is a strong mixture of the S $3p_z$ and F $2p_z$ orbitals at r_e. The GVB overlap of the bond pair at r_e is 0.78. The behavior in SF($^2\Pi$) is typical of polar covalent bonds: the GVB orbital on the more electronegative atom is largely unchanged by bond formation, while the GVB orbital on the less electronegative atom delocalizes onto the more electronegative atom. This corresponds to building (S^+)(F^-) character into the wave function.

The bonding orbitals in the $^4\Sigma^-$ excited state (Figure 3b) are both different from and similar to those of the ground state. In the natural orbital model, the doubly occupied 7σ orbital is localized on S at large separations, but it steadily delocalizes onto F as the internuclear distance decreases until it is essentially a polarized F orbital at r_e. In fact, it bears a fair resemblance to the natural σ bonding orbital from the ground state, although it retains somewhat more S character. While the doubly occupied orbital is changing in this manner, the singly occupied orbital (8σ) that begins as the unpaired electron on F delocalizes toward S and becomes a S−F antibonding orbital. It also resembles the corresponding antibonding orbital in the ground state, though it is now occupied by an electron instead of being only weakly occupied as in SF($^2\Pi$).

In the GVB model, the behavior of the orbitals during the formation of SF($^4\Sigma^-$) is very different and provides insight that is less evident in the natural orbital model. In the GVB wave function, there are orbitals for each of the three electrons. At $r_{SF} = \infty$, the electron from the F $2p_z$ orbital is in the 8σ orbital, while the S $3p_z^2$ singlet-coupled pair of electrons is split into left and right lobe orbitals ($7\sigma_L$, $7\sigma_R$), each with the larger part of its charge on opposite sides of the nucleus from each other. The orbital that is used to correlate the S $3p_{z^2}$ pair has $3d_{z^2}$ character, but the mixing of d character into the S $3p_z$ orbital is very small (much smaller than in Pauling's d-orbital hybridization theory). As the internuclear distance decreases, both of the lobe orbitals steadily delocalize from S onto F, while the 8σ orbital delocalizes the other direction, from F onto S. At r_e, the $7\sigma_R$ orbital very much resembles the singly occupied atomic F orbital at large separation (having exchanged places with the 8σ orbital) and it overlaps strongly (0.91) with the $7\sigma_L$ orbital. Together they constitute a bond pair similar to the polar covalent bond pair in SF($^2\Pi$) described above. The remaining electron is in the 8σ orbital, which resembles the original S lobe orbital ($7\sigma_R$) but has acquired considerable antibonding character.

As the plots of the orbitals demonstrate, the processes by which bonding occurs in SF($^2\Pi$) and in SF($^4\Sigma^-$) are distinctively different. The ground state is a typical polar covalent bond, where two electrons in singly occupied orbitals on each atom become singlet coupled, leading to a bound molecular state. The bonding in the $^4\Sigma^-$ state requires a *decoupling* of the singlet coupled S $3p_{z^2}$ pair of electrons and a subsequent *recoupling* of one of these electrons with the electron in the F $2p_z$ orbital to form a new covalent bond pair. This occurs in a smooth, continuous fashion as r decreases. While this mode of bonding forms a stable bond, there is a significant cost incurred by breaking up the pair of electrons, which results in the substantially weaker bond energy of the $^4\Sigma^-$ state.

The preceding discussion of the nature of bonding in SF($^4\Sigma^-$) lays the groundwork for a deeper understanding of hypervalency. Hypercoordination cannot occur unless electrons that are less available for molecular bonding—such as a pair of more deeply bound atomic electrons—are made available due to favorable energetics (this is essentially the democracy principle proposed by Cooper and co-workers[9]). The mechanism by which this occurs is the recoupling process described above. Recoupled pair bonding is therefore the hallmark of hypervalency. The coupling of SF($^4\Sigma^-$) is depicted in Figure 4. (As in all orbital coupling diagrams, the orbitals have a more complicated structure than this simplified iconography; see Figure 3.) As a consequence of recoupling the S $3p^2$ electrons, three unpaired electrons are available in SF($^4\Sigma^-$) to form hypercoordinated species such as SF_3 and SF_4. In fact, the geometrical dispositions of these three electrons provide the skeletal structure that will be adopted by SF_4, which has two equatorial and two axial SF bonds. Since the energetic cost of breaking up the pair of electrons has already been expended, subsequent bonds are expected to be much stronger than the SF($^4\Sigma^-$) bond energy. The results described below confirm this.

Finally, we conclude that SF cannot be classified as being either a covalent or hypervalent compound; *it is the nature of the bonding in a given state that matters*. The $^2\Pi$ state has a polar covalent bond, while the $^4\Sigma^-$ state has a hypervalent recoupled pair bond. In the larger SF_n species, we will find that different combinations of covalent and hypervalent bonding can occur within different states and can even coexist within the same species.

3.2. States of SF^+ and SF^-. Further insight into the nature of bonding in SF can be gained by examining the structural and energetic changes that occur when an electron is either

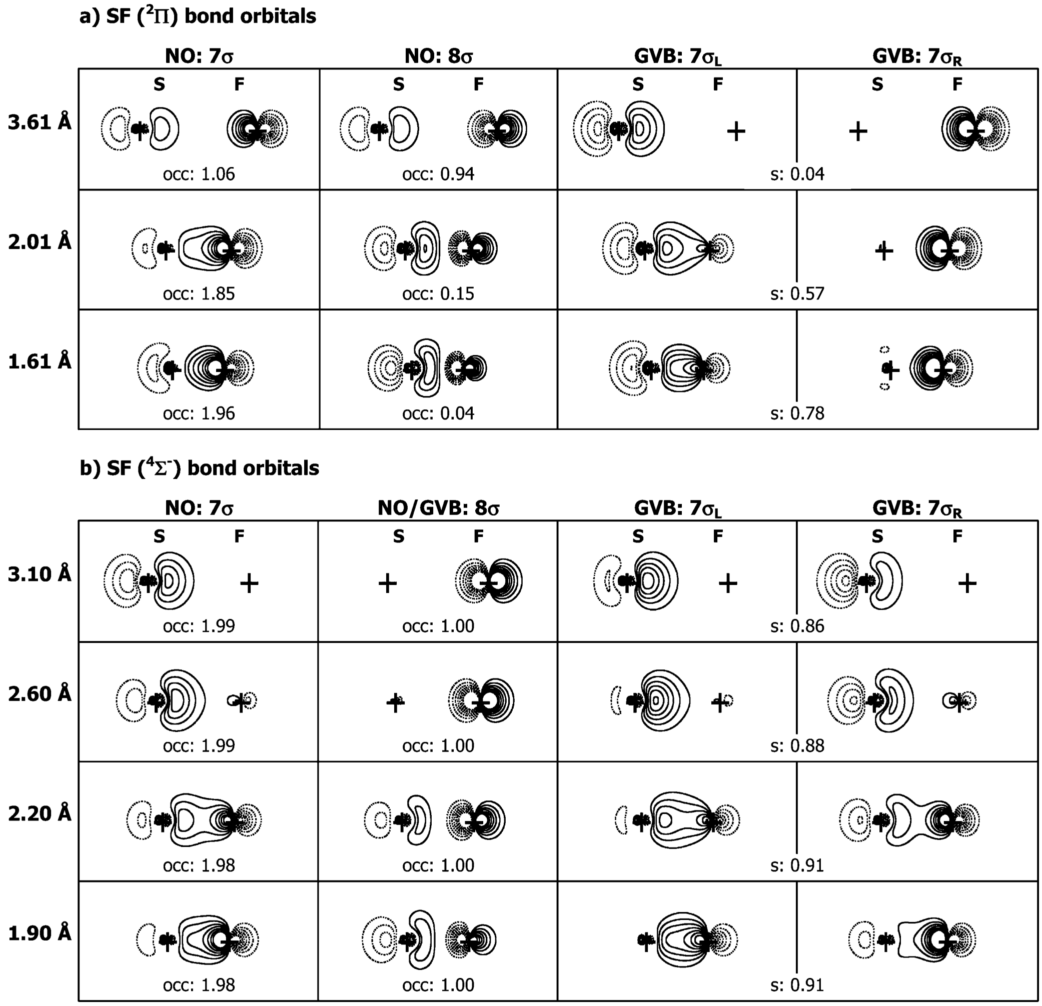

Figure 3. 2D sections of the bonding orbitals of the low-lying states of SF at various internuclear separations comparing natural orbitals (NO) and generalized valence bond (GVB) orbitals. Positions of the nuclei are indicated by + symbols. Contours are ±0.10, ±0.15, ±0.20, ±0.25, and ±0.30; positive amplitudes are represented by solid lines. Occupations (occ) and overlaps (s) are indicated for natural and GVB orbitals, respectively. (a) $^2\Pi$ state and (b) $^4\Sigma^-$ state.

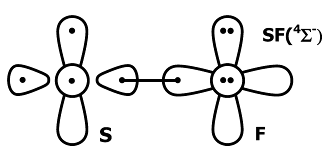

Figure 4. Orbital coupling diagram for $SF(^4\Sigma^-)$. The atomic $3p_z^2$ orbital of S has been decoupled into right and left lobe orbitals.

removed from or added to each of the states discussed above. Representative states for cations and anions that can be formed from the $^2\Pi$ and $^4\Sigma^-$ states of SF, and their respective ionization energies (IE) or electron affinities (EA) are depicted in Figure 5.

Removing an electron from $SF(^2\Pi)$ yields SF^+ in a $^3\Sigma^-$ or $^1\Delta$ state, depending on whether the electron is taken from the doubly or singly occupied π orbital. The respective calculated IEs are 10.04 and 11.07 eV. Measurements of the IE of ground state SF include 10.09 eV by Hildenbrand[33] and 10.16 ± 0.17 eV by Fisher et al.[34] Removing an electron from a π orbital reduces the SF bond length by about 0.09 Å, which is consistent with the weak S−F antibonding character associated with the orbital. The $^3\Sigma^-$ state of SF^+ can also be formed by removing the unpaired electron from the 8σ orbital of $SF(^4\Sigma^-)$, with a calculated IE of just 7.94 eV. Relative to $SF(^4\Sigma^-)$, removing this electron has an enormous impact on the SF bond length, decreasing it by 0.4 Å. It is therefore clear that the long bond length of $SF(^4\Sigma^-)$ is due to the presence of an electron in an orbital with pronounced antibonding character, as shown in Figure 3b. Not only does removing this electron result in a large reduction in bond length, the amount of energy needed to remove it is more than 2 eV less than the other IE values.

Similar behavior is observed when an electron is added to SF to form the SF^- anion, which has two bound states as previously noted in a computational study by Peterson and Woods.[44] If an electron is added to the singly occupied π orbital of $SF(^2\Pi)$ and $SF(^4\Sigma^-)$, the $^1\Sigma^+$ and $^3\Pi$ states of SF^- are formed with EA values of 2.20 and 2.73 eV, respectively. Each of these additions results in moderate increases in the bond length, of 0.12 and 0.23 Å, respectively. A much more dramatic change occurs if $SF^-(^3\Pi)$ is formed by adding an electron to the unoccupied 8σ antibonding orbital of $SF(^2\Pi)$. The EA for this is only 0.63 eV, and the bond length increases by more than 0.5 Å. Again, we see that partial occupation of the antibonding orbital significantly changes the bond length and incurs an additional energetic cost not present when the electron is added to a π orbital. Polak et al.[45] reported an experimental value for the EA of ground state SF of 2.285 ± 0.006 eV and found the bond length of ground state $SF^-(^1\Sigma^+)$ to be 1.717 ± 0.015 Å, values which are in good agreement with our calculated results.

3.3. Summary for SF. Accurate calculations for the low-lying states of SF demonstrate that it is energetically possible

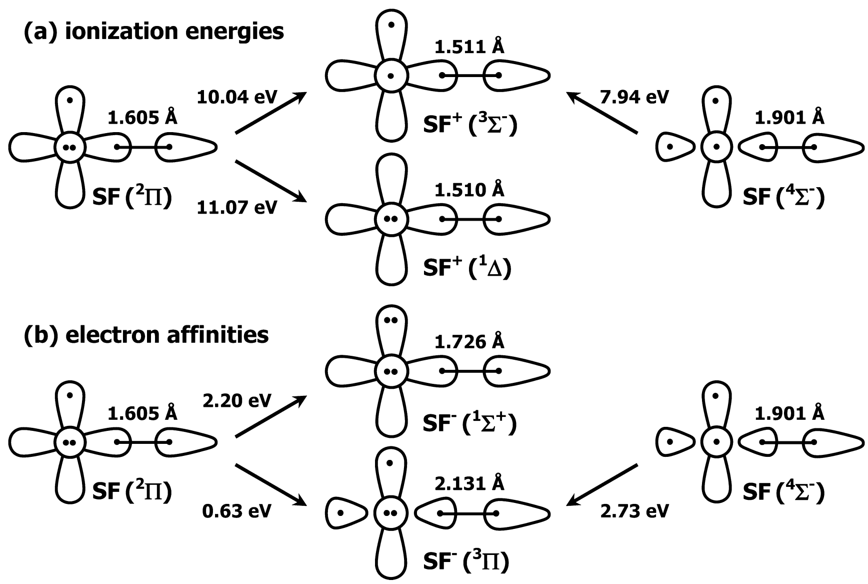

Figure 5. Orbital coupling diagrams, bond lengths, and relative energies of low-lying states of SF, SF^+, and SF^- at the MRCI+Q/AV5Z level. Energy differences include harmonic zero-point energy corrections. (a) Ionization energies and (b) electron affinities.

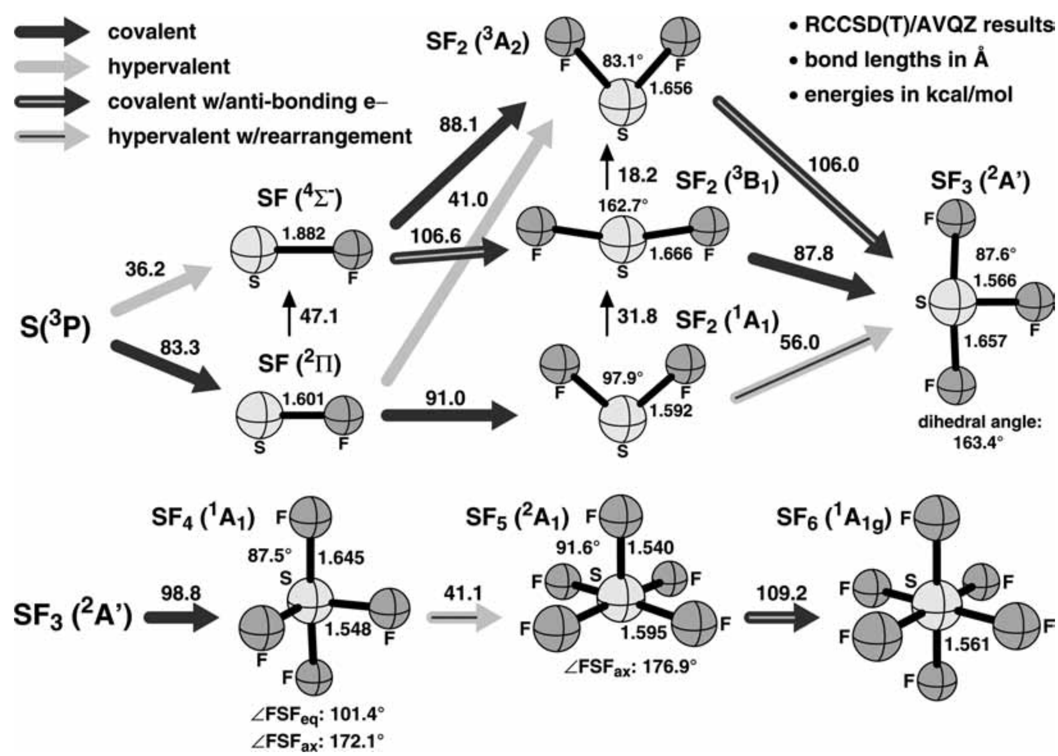

Figure 6. Formation pathways for SF_n species. Equilibrium bond dissociation energies (no zero-point energy corrections) are in kcal/mol, and bond lengths are in Å.

to form a bond either by simple covalent coupling of two unpaired electrons or by hypervalent recoupling involving three electrons. The $^2\Pi$ ground state of SF is bound by a strong polar covalent bond (~85 kcal/mol), while the first $^4\Sigma^-$ excited state[46] is bound by a weaker hypervalent bond (~35 kcal/mol). Because the $^4\Sigma^-$ state has an electron in a σ antibonding orbital, its bond energy is much smaller (by about 50 kcal/mol) and its bond length is much longer (by about 0.3 Å) than the corresponding values of the ground state properties. Calculations for states of SF^+ and SF^- confirm that an electron in the σ antibonding orbital lengthens the bond significantly and is much less tightly bound than the electrons in the valence π orbitals. In the following sections, we will show that what we have learned about the behavior of SF lays the groundwork for understanding the bonding in SF_2 and then SF_3 through SF_6.

4. Covalent and Hypervalent Bonding in SF_2

The remainder of this study will trace the various pathways by which SF_6 can be formed by subsequent additions of F to intermediate SF_n species, starting with adding F to SF to yield SF_2 in its ground and low-lying excited states. The structures and energetic changes at the RCCSD(T)/AVQZ level and subsequent F additions are summarized in Figure 6. We will see that there are clear patterns in the energetics, structures, and spectra of the remaining SF_n species that can be understood

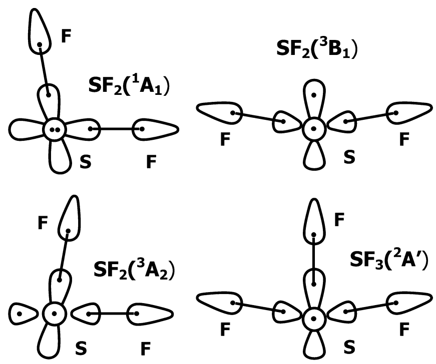

Figure 7. Orbital coupling diagrams for states of SF_2 and SF_3.

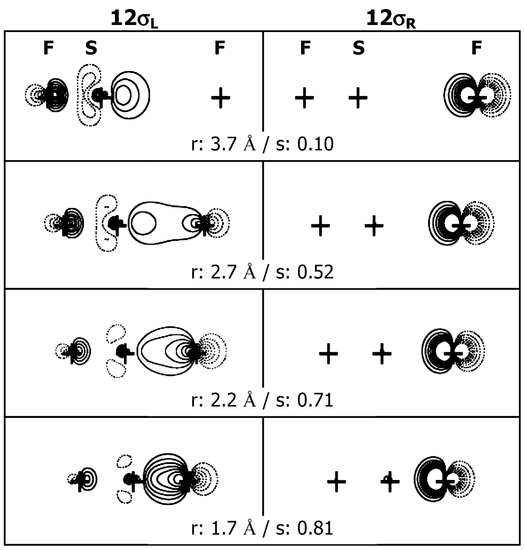

Figure 8. 2D sections of the GVB bonding orbitals during the formation of $SF_2(^3\Sigma^-)$ at various internuclear separations. Positions of the nuclei are indicated by + symbols. Contours are ±0.10, ±0.15, ±0.20, ±0.25, and ±0.30; positive amplitudes are represented by solid lines.

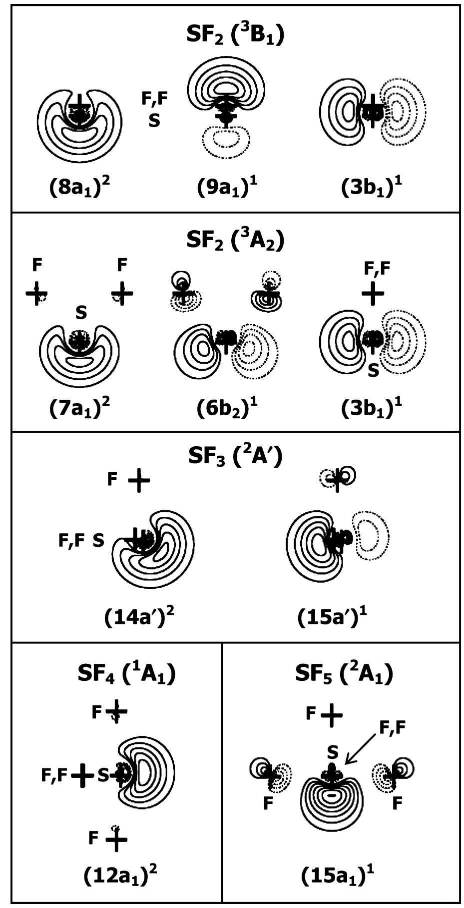

Figure 9. 2D sections of selected orbitals of SF_n species. Positions of nuclei are indicated by + symbols. Contours are ±0.10, ±0.15, ±0.20, ±0.25, and ±0.30; positive amplitudes are represented by solid lines.

as arising from the interplay between normal polar covalent and recoupled pair (hypervalent) bonds.

Triatomic SF_2 has multiple low-lying bound states that are formed by covalent or hypervalent additions of F to the $^2\Pi$ and $^4\Sigma^-$ states of SF. The dispositions of the orbitals with the unpaired electrons in those two states suggest possible states and structures for SF_2. Starting with ground state $SF(^2\Pi)$, one new structure can be formed via normal covalent coupling of its unpaired electron with one from a second F (see Figure 7), yielding a bent structure with $^1A_1$ symmetry and a bond angle close to 90° (97.9°). The second covalent bond energy (D_e) is 91.0 kcal/mol, about 10% larger than the bond energy of $SF(^2\Pi)$.[47] The equilibrium bond lengths in $SF_2(^1A_1)$ of 1.592 Å are only slightly shorter (about 0.01 Å) than the bond length of ground state SF. Endo et al.[48] reported structural parameters for ground state SF_2 of $r_e = 1.587\,45 \pm 0.000\,12$ Å and $\theta_e = 98.048 \pm 0.013°$.

Starting instead with $SF(^4\Sigma^-)$, two triplet states can be formed by covalently bonding F with either the electron in the σ orbital or one of the electrons in the two π orbitals (see Figure 7). The first of these additions yields a structure with a bond angle near 180° (a $^3\Sigma^-$ state if linear, $^3B_1$ if bent), while the other yields a $^3A_2$ state with a bond angle near 90°. The structures of the $^3B_1$ and $^3A_2$ states of SF_2 are shown in Figure 6, while their coupling diagrams are shown in Figure 7. The respective bond energies (D_e) of these states with respect to $SF(^4\Sigma^-)$ are 106.6 and 88.1 kcal/mol, and their respective bond angles are 162.7° and 83.1°. While the energy of the new bond in $SF_2(^3A_2)$ is similar to the two bond energies of $SF_2(^1A_1)$, the second bond in $SF_2(^3B_1)$ is *stronger* than these simple covalent bonds by about 15 kcal/mol.

What is the source of this additional bond energy? As noted previously, the long bond length of $SF(^4\Sigma^-)$ is due to the antibonding character of its singly occupied σ orbital. When a polar covalent bond is formed between the electron in this orbital and the unpaired electron in the 2p orbital of *very* electronegative F, the antibonding σ orbital delocalizes almost entirely onto the second F [see Figure 8 and S07 (Supporting Information)]. As a consequence, the antibonding character of the orbital decreases dramatically, which results in a commensurate increase (15 kcal/mol) in the bond energy and reduction (0.2 A) in the bond length. This mirrors what was observed above when the electron was removed from the σ antibonding orbital of $SF(^4\Sigma^-)$ to form $SF^+(^3\Sigma^-)$. Figure 8 also shows that the singly occupied orbital on F shifts only slightly toward S as the separation decreases, as seen above in $SF(^2\Pi)$.

The deviations of the bond angles of $SF_2(^3B_1)$ and $SF_2(^3A_2)$ from 180° and 90°, respectively, can be understood by examining a few orbitals for each of the states [see Figure 9 and S08 (Supporting Information)], including the two that are singly occupied and the one that is closely associated with the electrons in what was the $3s^2$ pair of S. In both states, one of the unpaired electrons is in an orbital ($3b_1$ in both cases) that still resembles a S 3p orbital, while the orbital with the $3s^2$ electrons from S are displaced significantly away from the nucleus to reduce the repulsion with the bond pairs. In $SF_2(^3B_1)$, the remaining singly occupied orbital ($9a_1$) is distorted away from the $3s^2$ pair ($8a_1$), and the bond angle is bent toward the singly occupied orbital. In spite of the large displacement of the bond angle from 180°, it is noteworthy that the bent configuration is only 0.4 kcal/mol lower in energy than the linear $^3\Sigma^-$ (transition) state, where the S $3s^2$ pair is constrained to be centered on the S nucleus and thus wedged between the two bonds.

In $SF_2(^3A_2)$, the other singly occupied orbital ($6b_2$) and the $3s^2$ pair ($7a_1$) both lie in the plane of the molecule and compress the bond angle to 83.1°. The $6b_2$ orbital of $SF_2(^3A_2)$ is antibonding, which accounts for why the state lies 18.2 kcal/mol higher in energy than the $^3B_1$ state (where the antibonding electron from the recoupling has been incorporated into a polar covalent bond).

There is one more pathway of interest, the formation of $SF_2(^3A_2)$ via hypervalent recoupled pair bonding, which occurs if the second F interacts with the pair of electrons in the π orbital in the $^2\Pi$ ground state instead of with its unpaired electron (see Figure 7). The energy of this bond (41.0 kcal/mol) is similar to the hypervalent bond energy in $SF(^4\Sigma^-)$ (36.2 kcal/mol), and the difference (50.0 kcal/mol) between the covalent and hypervalent additions to form $SF_2(^1A_1)$ and $SF_2(^3A_2)$, respectively, is similar to the state separation in SF (47.1 kcal/mol).

Experimental values for the geometry of $SF_2(^1A_1)$ include studies by Johnson and Powell[49] ($r_0 = 1.589$ Å, $\theta_0 = 98.27°$), Kirchhoff et al.[50] ($r_0 = 1.592\,08 \pm 0.000\,08$ Å, $\theta_0 = 98.197 \pm 0.011°$), and Endo et al.[48] ($r_0 = 1.587\,45 \pm 0.000\,12$ Å, $\theta_0 = 98.048 \pm 0.013°$), which are in reasonable agreement with our equilibrium values ($r_e = 1.592$ Å; $\theta_e = 97.7°$). With ZPE corrections, our calculated value for D_0 of $SF_2(^1A_1)$ is 89.5 kcal/mol. Kiang and Zare[17] reported a value of $D_0 = 91.7 \pm 4.3$ kcal/mol for the SF−F bond energy in ground state SF_2, while a value of $D_0 = 94.3 \pm 4.6$ kcal/mol was reported by Fisher et al.[34] Previous high-level theoretical predictions for the $SF_2 \rightarrow SF + F$ dissociation energy (ground state) are shown in Table 1. Our RCCSD(T)/AVTZ value of the dipole moment for the ground state is $\mu_e = 1.11$ D, in very good agreement with the measured value of $\mu_e = 1.05$ D reported by Johnson and Powell.[49] The predicted values of μ_e for the $^3B_1$ and $^3A_2$ states are 0.35 and 1.78 D, respectively.

Most of the previous theoretical studies of SF_2 have focused on the ground state. Although two recent studies[51] have treated the excited singlet states of SF_2, only Yu et al.[52] and Ziegler and Gutsev[21] characterized the triplet states. The structures and relative energies for the $^1A_1$, $^3B_1$, and $^3A_2$ states reported in the latter paper are roughly comparable to the ones in our study. Both papers attribute the small bond angle of the $^3A_2$ state to antibonding character in the singly occupied b_2 orbital. While the 1977 study of Hay[53] does not discuss SF_2 excited states, its discussion of bonding in SF_2 and SF_4 in terms of GVB orbitals parallels our treatment in many respects (and anticipated it by three decades).

5. Covalent and Hypervalent Bonding in SF_3 through SF_6

5.1. SF_3. SF_3 has only a single low-lying state ($^2A'$), but it can be formed from each of the three states of SF_2 described above (see Figure 6). Its coupling diagram is shown in Figure 7. Addition to the two triplet state structures is straightforward; addition to $SF_2(^1A_1)$ will be discussed below. If the third F forms a bond with one of the unpaired electrons of $SF_2(^3B_1)$, a simple covalent bond of 87.8 kcal/mol (D_e) is formed, which falls in the same range as the other three simple covalent bonds discussed previously. If another F is added to $SF_2(^3A_2)$, the energetic penalty incurred by the electron in its antibonding orbital is mitigated (as seen previously when forming $SF_2(^3B_1)$ from the $^4\Sigma^-$ state of SF), yielding a SF bond energy (D_e) of 106.0 kcal/mol.

The length of the two axial SF bonds of SF_3 is about 0.01 Å less than the bond length in $SF_2(^3B_1)$, while the length of its equatorial covalent bond is about 0.03 Å less than the length of the polar covalent bond in $SF_2(^1A_1)$. The bond angle between the axial SF bonds of SF_3 is 162.8°, which is very close to the value noted above for $SF_2(^3B_1)$. As shown in Figure 9, the small nonplanarity of SF_3 (163.4° dihedral angle) reflects a balance between the influence of the doubly occupied orbital (14a′) associated with the S $3s^2$ electron pair and the singly occupied orbital (15a′) (see also S09, Supporting Information) The orbitals lie on opposite sides of the approximate plane of the molecule, and the distortion, as expected, is toward the singly occupied orbital. (Baird et al.[54] offered arguments similar to ours to explain the structures of SF_3 and SF_5.) In spite of the small deviation from planarity, the out-of-plane component of the dipole moment was computed to be $\mu_e = 0.433$ D at the RCCSD(T)/AVTZ level. The in-plane component is 0.699 D, yielding a net dipole moment (μ_e) of 0.822 D.

The final pathway to the formation of SF_3 is the addition of F to $SF_2(^1A_1)$. This process introduces another variation on the bonding modes of SF_n. As in the formation of $SF(^4\Sigma^-)$, the S $3p^2$ pair is recoupled to free up an electron to bond with F. The reduced bond energy (D_e) of 56.0 kcal/mol reflects the energetic cost of the recoupling, as observed in previous hypervalent additions. However, this bond energy is 15−20 kcal/mol larger than the two hypervalent recoupled pair bonds encountered previously. The difference is that the bonding in SF_3 rearranges once the recoupling has occurred to alleviate the energetic cost associated with introducing an antibonding electron. Ground state SF_2 has two covalent bonds that do not involve antibonding electrons, while SF_3 has one normal covalent bond and two bonds that involve the recoupled pair. This rearrangement is clearly favored energetically.

The nature of bond formation in $SF_2(^1A_1) + F$, recoupling and simultaneous bond rearrangement, can be seen in the manner in which both the geometry and the orbitals change as the F approaches SF_2. We explored this process with constrained optimizations at the RCCSD(T)/AVTZ level followed by MCSCF calculations with a limited active space (three electrons in orbitals 21a−23a, with the last one a virtual orbital, and all of the other valence orbitals constrained to be doubly occupied). Figure 10 depicts snapshots of orbitals 21a and 22a, which are doubly and singly occupied in SF_3, at various separations (for animations, see S10 in the Supporting Information). The dihedral angles are also noted. The F begins by attacking the S lone pair orbital dominated by S $3p^2$ character, at a dihedral angle around 100°, and then swings down toward the plane as the bond length decreases below about 2.45 Å. In SF_3, it has moved to a position nearly 180° from one of the two covalently bonded F atoms. Together, these two bonds constitute a pair of recoupled pair bonds like the ones in $SF_2(^3B_1)$. As in the formation of $SF(^4\Sigma^-)$, no barrier is encountered for this addition. The progression clearly shows that the singly occupied orbital (22a) is localized on F at large r_{SF} and shifts to being localized on S in SF_3, while the doubly occupied orbital (21a) is initially localized on S and becomes the new SF bond pair in SF_3. The change is remarkable given both the spatial displacement and the change in orientation that occurs in both orbitals.

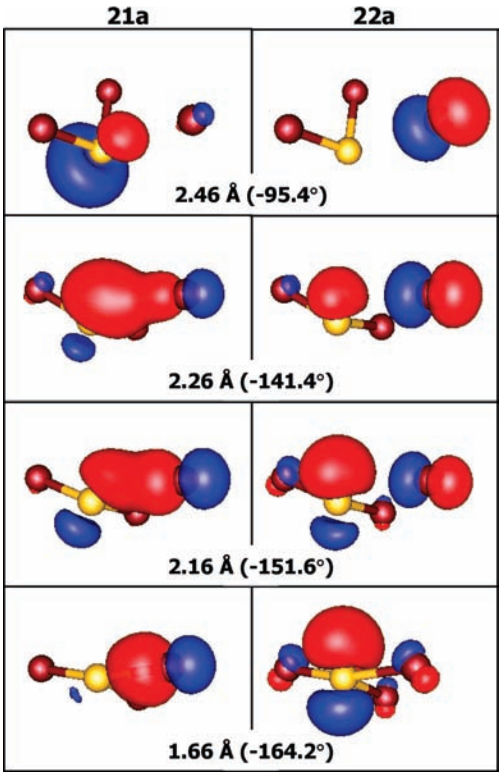

Figure 10. Snapshots of the 21a and 22a natural orbitals at various r_{SF} distances for F addition to $^1A_1$ SF_2 to form $^2A'$ SF_3. Dihedral angles are given in parentheses. Structures are from a constrained optimization, as described in the text.

Following an early ESR study by Colussi et al.[55] which found that SF_3 has a single symmetry plane and two types of SF bonds, Kiang and Zare[17] reported a very approximate value of $D_0 = 63.1 \pm 7.1$ kcal/mol for the SF_2−F bond energy in SF_3, while a value of $D_0 = 60.9 \pm 2.8$ kcal/mol was reported by Fisher et al.[33] Our prediction of D_0 for this bond is 54.5 kcal/mol (see Table 1 for previous high level theoretical predictions). No experimental structure or dipole moment has been reported for SF_3 to date, evidently due to the very brief lifetime of the radical.

5.2. SF_4. The $^1A_1$ ground state of SF_4 is formed straightforwardly (see Figure 6) by covalent addition of F to $SF_3(^2A')$. The polar covalent (eq) and recoupled pair (ax) bond lengths, 1.548 and 1.645 Å, respectively, have contracted by about 0.02 and 0.01 Å, respectively, from their values in $SF_3(^2A')$. The bond angles of 101.4° (eq) and 172.1° (ax) are similar or increase slightly in response to the addition of a fourth bond pair. The orbital dominated by the S 3s atomic orbital ($12a_1$) is depicted in Figure 9; it is once again displaced from the S nucleus (see also S09, Supporting Information). The repulsive interaction between the lone pair and the four bond pairs of the axial F atoms pushes the latter onto the same side of the molecule as the equatorial F atom. While the largest coefficient of the $12a_1$ orbital is from the S 3s basis function, there is also a large S 3p contribution, indicating that significant hybridization has occurred.

Structural parameters for $SF_4(^1A_1)$ were determined by Tolles and Gwinn[56] as follows: $r_{SF}(\text{eq}) = 1.545 \pm 0.003$, $r_{SF}(\text{ax}) = 1.646 \pm 0.003$ Å, $\theta_{FSF}(\text{eq}) = 101.55 \pm 0.5°$, and $\theta_{FSF}(\text{ax}) = 173.07 \pm 0.5°$. They also reported $\mu_0 = 0.632 \pm 0.003$ D, which is very similar to our computed μ_e value of 0.658 D. Kiang and Zare[17] and Fisher et al.[33] reported D_0 values of 84.1 ± 3.0 and 89.2 ± 2.3 kcal/mol, respectively, for the SF_3−F bond energy in SF_4. Our calculated value for D_0 is 96.2 kcal/mol (see Table 1 for previous high level theoretical results).

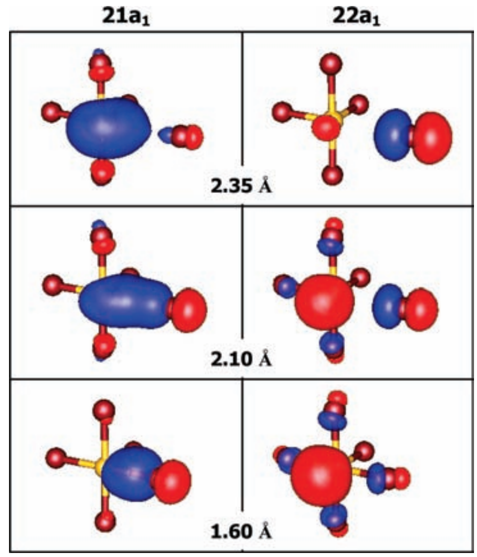

Figure 11. Snapshots of the $21a_1$ and $22a_1$ natural orbitals at various r_{SF} distances for F addition to $^1A_1$ SF_4 to form $^2A_1$ SF_5. Structures are from an unoptimized scan, as described in the text.

In addition to the minimum structure, there is a transition state (saddle point) of SF_4 with C_{4v} symmetry that corresponds to interconversion of the pairs of covalent and recoupled-pair bonds. Its four equivalent SF bond lengths are 1.606 Å, and the bond angle between F atoms on the opposite sides of S are 140.1°. This structure lies 11.0 kcal/mol (ΔE_e) above the minimum and likely owes its stability to the favorable energetics of forming a second pair of recoupled-pair bonds (anticipating SF_5). Initial experimental evidence for the C_{2v} structure of SF_4 includes studies by Dodd et al.[57] and Cotton et al.[58] On the basis of temperature dependence of chemical shifts and nuclear spin coupling constants, Muetterties and Phillips[59] reported a value of 4.5 ± 0.8 kcal/mol for the activation energy for F exchange in SF_4.

5.3. SF_5 and SF_6. Adding F to SF_4 yields SF_5 in its $^2A_1$ ground state (see Figure 6). Like F addition to $SF_2(^1A_1)$, this process involves both the recoupling of electrons (the pair that began as the $3s^2$ electrons of atomic S) and subsequent rearrangement of bonding, forming a set of recoupled bond pairs with one of the two covalent bonds in SF_4. The calculated energy (D_e) of the fifth SF bond is 41.1 kcal/mol. The four F atoms that lie nearly in a plane participate in two pairs of recoupled-pair bonds, with $r_e = 1.595$ Å, while the final SF bond length has decreased to 1.540 Å.

We examined the nature of F addition to $SF_4(^1A_1)$ with a simple 1D scan with a limited CASSCF wave function in which the bond length for one of the four equivalent F atoms was increased in a stepwise manner while the remainder of the geometry was left unchanged. Snapshots of the orbitals involved in the recoupling are depicted in Figure 11 (for animations, see S11 in the Supporting Information). As in the hypervalent additions to S and SF_2, the locations and character of the singly occupied ($22a_1$) and doubly occupied ($21a_1$) orbitals shift as the F approaches. The remaining S lone pair becomes the new S−F bond pair, while the unpaired electron moves from F to S. Once again, the net effect is to recouple the atomic pair. While it remains uninvolved in bonding in the smaller SF_n species, the second S lone pair acquires more and more p hybridization as polar bond pairs fill in around S. The singly occupied orbital in SF_5 has more p than s character [see Figure 9 and S09 (Supporting Information)].

Observations of SF_5 date back to an EPR study by Morton and Preston[60] and an earlier ESR study by Fessenden and Schuler[61] reinterpreted by Morton and Preston. Like SF_3, SF_5 is very reactive, and no experimental structure or dipole moment has been reported to date. Our computed value for the dipole moment (μ_e) is 0.311 D. Kiang and Zare[17] and Fisher et al.[34] reported respective D_0 values of 53.1 ± 6.0 and 57.9 ± 3.0 kcal/mol for the SF_4−F bond energy in SF_5. Our calculated value of D_0 is 39.2 kcal/mol, which is consistent with the previous high level theoretical predictions (see Table 1). The very large difference between the high-level theoretical and the experimental values of D_0 suggests possible difficulties with the latter.

Octahedral SF_6 is formed by covalently bonding F to the electron in the singly occupied orbital ($15a_1$) of SF_5, which lies below the plane of the axial SF bonds, as shown in Figure 9. The RCCSD(T)/AVQZ value for this bond energy (D_e) is 109.2 kcal/mol and r_{SF} is 1.561 Å. It is the strongest of the incremental bond energies and is of similar strength as the other two covalent bonds involving an electron in an orbital with antibonding character and completes the final of three pairs of linear or quasilinear F−S−F bond pairs (notable given that only two recoupling events must occur at some point in the path, one for SF_3 and the other for SF_5).

Following the first report of SF_6 formation by Moissan,[18] various experimental studies reported values for the bond length and SF_5−F bond energy. Experimental values for r_0 in SF_6 include 1.58 ± 0.03 Å by Brockway and Pauling[62] and 1.564 ± 0.010 by Ewing and Sutton.[63] Values of D_0 for SF_5−F include 89.9 ± 3.4 kcal/mol by Kiang et al.,[64] 91.1 ± 3.2 kcal/mol by Kiang and Zare,[17] 94.5 ± 3.0 kcal/mol by Babcock and Streit,[65] and 100.4 ± 2.4 kcal/mol by Tsang and Herron.[66] As Tsang and Herron[66] and Irikura[36] have summarized, there has been controversy regarding the experimental values for the bond energy; theory (including the present work) consistently predicts larger values than experiment. Our calculated value of D_0 is 105.6 kcal/mol (see Table 1 for previous high level theoretical results).

6. Recoupled Pair Bonding in the CH_n ($n = 1, 4$) Series

While it is instructive to discuss the bonding in the SF_n species as a combination of normal covalent and recoupled pair bonding of sulfur's $3p^2$ and then $3s^2$ electrons, the same underlying behavior has been observed in atoms that have not generally been considered to be hypervalent. In fact, Be, B, and C (and their heavier cousins in the periodic table) all participate in diatomic and larger species where at least some of the low-lying bound states depend upon recoupling the $2s^2$ pair of the atoms. For the most part, beryllium cannot form covalent bonds without recoupling its $2s^2$ pair, while BH and CH each have very low-lying states ($^3\Pi$ and $^4\Sigma^-$, respectively) that also involve recoupling their $2s^2$ pairs. Recoupling is so favorable in C that the $^3B_1$ state of CH_2 lies below the $^1A_1$ state and opens the door for carbon's predominant tetravalence in larger species. If recoupled pair bonding is the hallmark of hypervalency, then beryllium, boron, and carbon are as prone to hypervalent behavior (or more so!) as phosphorus, sulfur, chlorine, and xenon.

It should be noted that there are critical differences between recoupling in C and S. Sulfur only forms hypervalent bonds with atoms or radicals with large electron affinities that are able to pull charge away from it, decoupling its lone pairs of electrons. Hence, $SF(^4\Sigma^-)$ is stable but $HS(^4\Sigma^-)$ is not. The comparable ease with which $2s^2$ recoupling occurs in carbon is due to the s−p near degeneracy and the availability of an unoccupied p orbital, which readily allows hybridization to occur and results in two lobe orbitals that are spatially well-separated.[67] As a consequence, the cost of recoupling the pair of electrons is much smaller in C than in S, and C can therefore form recoupled pair (hypervalent) bonds with atoms with much lower electronegativities, such as H. The energy of the recoupled pair bond in $CH(^4\Sigma^-)$ is 67.2 kcal/mol, which is just 16.7 kcal/mol less than the bond energy of ground state $CH(^2\Pi)$, 83.9 kcal/mol.[68] As noted above, the differences between covalent and hypervalent bond energies in S compounds [$SF(^2\Pi)/SF(^4\Sigma^-)$, $SF_2(^1A_1)/SF_2(^3A_2)$] were much larger, about 50 kcal/mol.

While they did not use the same terminology and did not make the connection to hypervalency in compounds of P, S, Cl, and related elements, studies by Goddard and co-workers[30,69] investigated s^2 recoupling in compounds of B, C, Si, and other elements. Their description is essentially equivalent to ours and merits acknowledgment.

As Musher proceeded through his seminal exploration of hypervalency,[10] there are indications that he may have been laying the groundwork for reformulating fundamental bonding concepts along some of the same lines we suggest here. There are hints he was thinking beyond the elements he identified as hypervalent (HV, in his usage). Due to his untimely passing, his contributions to the subject were limited to a few additional papers.[70] But there are tantalizing clues in his initial study,[10] such as when he writes (p 57) "Notice that in this sense methane is like an HV molecule in that it requires use of its atomic s electrons and electronic reorganization, or hybridization, it possesses a structure of the highest possible symmetry, and does not easily undergo chemical reactions...". He also describes hypervalency as an uncoupling process (p 59), when he compares the behavior to covalent bonding: "An electronic affinity, of course, must exist for the formation of ordinary covalent bonds, but must be significantly greater here in order to be able to decouple and delocalize the paired electrons in the donor atom of the already stable molecule."

7. Conclusions

This work has introduced a new theoretical model for hypervalency as a consequence of examining the low-lying states of all of the intermediate species that are precursors to stable hypercoordinated species such as SF_4 and SF_6. From this atom-by-atom approach, we concluded that hypervalent bonding is a distinct bonding process that differs fundamentally from simple covalent bonding: it occurs when it is energetically favorable to *recouple* an existing pair of electrons in order to form a new molecular bond with another atom. There is a cost associated with breaking up the pair of electrons, but this cost and more is recouped when another bond is formed using the second electron.

From our analysis of bonding in the ground and low-lying excited states of SF_n species, we were able to draw various conclusions about their energetics, structure, and spectra.

7.1. Energetics. We have shown that there are four distinct but interrelated bonding processes at work in SF_n, each of which is characterized by distinct bond energies (in parentheses): (1) simple covalent coupling (about 85−90 kcal/mol), (2) hypervalent recoupling (about 35−40 kcal/mol), (3) covalent coupling with an electron in the antibonding orbital from a recoupled pair bond (about 105−110 kcal/mol), and (4) hypervalent recoupling with simultaneous bond rearrangement (about 55 kcal/mol for the first pair of electrons, about 40 kcal/mol for the second pair).

7.2. Structure. The angle between covalent bonds is about 90°, while pairs of bonds arising from a hypervalent recoupling tend to be linear or quasilinear. For each radical species, the dispositions of the unpaired electrons were found to provide valuable clues about the structures of larger members of the series. While the nonbonding electrons influence structure, their impact is generally more subtle than suggested by other models.

7.3. Spectra. Low-lying bound excited states were found for both $SF(^4\Sigma^-)$ and $SF_2(^3B_1, {}^3A_2)$ that involve recoupled pair bonding. The $^4\Sigma^-$ excited state of SF is the first example of a recoupled pair (hypervalent) bond in the SF_n series, while the $^3B_1$ and $^3A_2$ states of SF_2 have both hypervalent and covalent bonds. The covalent bond in $SF_2(^3B_1)$ is stronger than the one in $SF_2(^3A_2)$ because it uses the electron in the antibonding orbital of $SF(^4\Sigma^-)$. If any of these excited states can be formed in the laboratory, they might be expected to have fairly long lifetimes given that they have different multiplicities than their respective ground states.

The oscillation of the SF_n−F bond energies for SF through SF_6 was recognized initially by Hildenbrand[33] and then discussed later by Kiang and Zare,[17] Cheung et al.,[35] and others. The behavior was attributed to the inherent stability of even-electron systems over odd-electron systems and to the implied cost of hybridization, particularly when F is added to SF_2 and SF_4. Our work has revealed that the energetic cost for addition to SF_n species with even n (including $n = 0$ in the case of the formation of the $^4\Sigma^-$ state of SF) is a direct consequence of disrupting stable singlet electron couplings as a trade-off for forming a new bond, while the bond energies associated with addition to SF_n with odd n are larger because that cost has already been expended and the unpaired electrons that participate in the bonds are in energetically unfavorable antibonding orbitals [except for $SF(^2\Pi)$ + F]. The bonding in both SF_3 and SF_5 rearranges to minimize the number of electrons in antibonding orbitals and thus maximize the number of quasilinear F−S−F recoupled pair bonds.

There is some commonality between the model we have described and the Rundle−Pimentel 3c/4e model. Many cases of hypervalent bonding do involve four electrons contributed by three centers. But there is limited predictive value in the 3c/4e model, because it does not account for the driving force that leads to hypervalent bonding. It does not provide sufficient insight to explain why some elements are hypervalent while others are not or to predict trends when comparing elements. The recoupled pair bonding model provides a more fundamental and coherent explanation for why hypervalency occurs and allows analysis and prediction that the 3c/4e model does not provide.

Much remains to be understood about the details of hypervalent recoupled pair bonding, such as characterizing the similarities and differences between p^2 electron pair recoupling in S and the other elements on the right side of the p-block and s^2 electron recoupling in C and the other elements on the left side of the p-block. Another topic of interest is why S readily forms hypervalently bound species while O does not, which we have investigated in a separate study[71] of the diatomic chalcogen halides (combinations of O, S, and Se with F, Cl, and Br). We will compare trends in SF_n and ClF_n species in an upcoming publication (Chen, Woon, and Dunning, in preparation). It is also evident that there is some threshold electronegativity that must be exceeded for hypervalent p^2 recoupling to occur: while a very electronegative atom such as F will induce S to recouple a p^2 electron pair, H, which has a much smaller electronegativity, will not. What is the threshold for a given pair of electrons in S to allow recoupling? Is there a way to predict trends for element/species X interacting with element/species Y based upon the particular properties of X and Y? Finally, it is expected that the reactivity of species containing P, S, Cl, and their cousins lower in the periodic table will be greatly influenced by the ability of these elements to form recoupled pair bonds. We have begun to explore a few of these reactions.

Acknowledgment. Support for this work was provided by funding from the Distinguished Chair for Research Excellence in Chemistry at the University of Illinois at Urbana−Champaign. We acknowledge the helpful insights from many people who listened to us as we assembled the pieces of this story and are particularly grateful for those who read the manuscript and offered helpful comments, including Prof. Kirk Peterson, Dr. Agnes Derecskei-Kovacs, and Dr. Lina Chen. This work is dedicated to the memory of J. I. Musher. We appreciate the reminiscences of Prof. Donald R. Beck of Michigan Technological University and Prof. Martin Pomerantz of the University of Texas at Arlington regarding Prof. Musher. Prof. Reggie L. Hudson of Eckerd College drew our attention to the ESR studies of Prof. T. F. Williams of the University of Tennessee.

Supporting Information Available: More detailed tables of parameters for SF and its ions and SF_2 through SF_6, as well as a more complete bibliography of experimental and prior theoretical studies of SF_n species and a PowerPoint file containing the animations mentioned in the text. This information is available free of charge via the Internet at http://pubs.acs.org.

References and Notes

(1) Pauling, L. *J. Am. Chem. Soc.* **1931**, *53*, 1367.

(2) (a) Pitzer, K. S. *Science* **1963**, *139*, 414. (b) Brown, R. D.; Peel, J. B. *Aust. J. Chem.* **1968**, *21*, 2605. 1968, *21*, 2617. (c) Kutzelnigg, W. *Angew. Chem., Int. Ed.* **1984**, *23*, 272. (d) Reed, A. E.; Weinhold, F. *J. Am. Chem. Soc.* **1986**, *108*, 3586. (e) Reed, A. E.; Schleyer, P. v. R. *J. Am. Chem. Soc.* **1990**, *112*, 1434. (f) Magnusson, E. *J. Am. Chem. Soc.* **1990**, *112*, 7940. (g) Pacchioni, G.; Bagus, P. S. *Inorg. Chem.* **1992**, *31*, 4391. (h) Glendening, E. D.; Badenhoop, J. K.; Weinhold, F. *J. Comput. Chem.* **1998**, *19*, 628.

(3) Gilheany, D. G. *Chem. Rev.* **1994**, *94*, 1339.

(4) Cooper, D. L.; Cunningham, T. P.; Gerratt, J.; Karadakov, P. B.; Raimondi, M. *J. Am. Chem. Soc.* **1994**, *116*, 4414.

(5) Gillbro, T.; Williams, F. *J. Am. Chem. Soc.* **1974**, *96*, 5032.

(6) Rundle, R. E. *J. Am. Chem. Soc.* **1947**, *69*, 1327. *J. Am. Chem. Soc.* **1963**, *85*, 112.

(7) Pimentel, G. C. *J. Chem. Phys.* **1951**, *19*, 446.

(8) (a) Harcourt, R. D. *J. Chem. Educ.* **1968**, *45*, 779. (b) Harcourt, R. D. *Int. J. Quantum Chem.* **1996**, *60*, 553. (c) Curnow, O. J. *J. Chem. Educ.* **1998**, *75*, 910. (d) Gillespie, R. J.; Robinson, E. A. *Inorg. Chem.* **1995**, *34*, 978. (e) Noury, S.; Silvi, B.; Gillespie, R. J. *Inorg. Chem.* **2002**, *41*, 2164. (f) Gillespie, R. J.; Silvi, B. *Coord. Chem. Rev.* **2002**, *233−234*, 53. (g) Cioslowski, J.; Surján, P. R. *J. Mol. Struct. Theochem* **1992**, *255*, 9. (h) Cioslowski, J.; Mixon, S. T. *Inorg. Chem.* **1993**, *32*, 3209. (i) Ponec, R.; Duben, A. J. *J. Comput. Chem.* **1999**, *20*, 760. (j) Ponec, R.; Gironés, X. *J. Phys. Chem. A* **2002**, *106*, 9506.

(9) (a) Cunningham, T. P.; Cooper, D. L.; Gerratt, J.; Karadakov, P. B.; Raimondi, M. *Int. J. Quantum Chem.* **1996**, *60*, 393. (b) Cunningham, T. P.; Cooper, D. L.; Gerratt, J.; Karadakov, P. B.; Raimondi, M. *J. Chem. Soc. Faraday Trans.* **1996**, *93*, 2247. (c) Karadakov, P. B.; Cooper, D. L.; Gerratt, J. *Theor. Chem. Acc.* **1998**, *100*, 222. (d) Cooper, D. L.; Gerratt, J.; Raimondi, M. In *Pauling's Legacy—Modern Modelling of the Chemical Bond*; Maksic, Z. B., Orville-Thomas, W. J., Eds.; Elsevier: Amsterdam, 1999; p 537. (e) Cooper, D. L. *Theor. Chem. Acc.* **2001**, *105*, 323.

(10) Musher, J. I. *Angew. Chem., Int. Ed.* **1969**, *8*, 54.

(11) Schleyer, P. v. R. *Chem. Eng. News* **1984**, *62*, 4.

(12) (a) Bartlett, N. *Proc. Chem. Soc.* **1962**, 218. (b) Hoppe, R.; Dähne, W.; Mattauch, H.; Rödder, K. *Angew. Chem., Int. Ed.* **1962**, *1*, 599. (c) Claassen, H. H.; Selig, H.; Malm, J. G. *J. Am. Chem. Soc.* **1962**, *84*, 3593. (d) Malm, J. G.; Sheft, I.; Chernick, C. L. *J. Am. Chem. Soc.* **1963**, *85*, 110. (e) Weaver, E. E.; Weinstock, B.; Knop, C. P. *J. Am. Chem. Soc.* **1963**, *85*, 111.

(13) Davy, H. *Philos. Trans.* **1810**, *100*, 231.

(14) Mitchell, K. A. R. *Chem. Rev.* **1969**, *69*, 157.

(15) Jensen, W. B. *J. Chem. Educ.* **2006**, *83*, 1751.

(16) McGrady, G. S.; Steed, J. W. Hypervalent Compounds. In *Encyclopedia of Inorganic Chemistry 2*; King, R. B., Ed.; John Wiley and Sons: Chichester, 2006 (doi: 10.1002/0470862106.ia094).

(17) Kiang, T.; Zare, R. N. *J. Am. Chem. Soc.* **1980**, *102*, 4024.

(18) (a) Moissan, H.; Lebeau, P. *Compt. Rend.* **1900**, *130*, 865. (b) Moissan, H. *Le Fluors et ses Composés*; G. Steinheil: Paris, 1900; pp 122–123.

(19) Keller, H. F. *J. Franklin Inst.* **1901**, *152*, 123.

(20) Tressaud, A. *Angew. Chem., Int. Ed.* **2006**, *45*, 6792.

(21) Ziegler, T.; Gutsev, G. L. *J. Chem. Phys.* **1992**, *96*, 7623.

(22) Werner, H.-J.; Knowles, P. J.; et al. *Molpro, Version 2002.6*; University College Cardiff Consultants Ltd.: Cardiff, U.K., 2004 (see Supporting Information for the complete reference).

(23) (a) Werner, H.-J.; Knowles, P. J. *J. Chem. Phys.* **1985**, *82*, 5053. (b) Knowles, P. J.; Werner, H.-J. *Chem. Phys. Lett.* **1985**, *115*, 259.

(24) (a) Werner, H.-J.; Knowles, P. J. *J. Chem. Phys.* **1988**, *89*, 5803. (b) Knowles, P. J.; Werner, H.-J. *Chem. Phys. Lett.* **1988**, *145*, 514.

(25) (a) Langhoff, S. R.; Davidson, E. R. *Int. J. Quantum Chem.* **1974**, *8*, 61. (b) Davidson, E. R.; Silver, D. W. *Chem. Phys. Lett.* **1977**, *52*, 403.

(26) (a) Purvis, G. D. III.; Bartlett, R. J. *J. Chem. Phys.* **1982**, *76*, 1910. (b) Raghavachari, K.; Trucks, G. W.; Pople, J. A.; Head-Gordon, M. *Chem. Phys. Lett.* **1989**, *157*, 479. (c) Knowles, P. J.; Hampel, C.; Werner, H.-J. *J. Chem. Phys.* **1993**, *99*, 5219. (d) Watts, J. D.; Gauss, J.; Bartlett, R. J. *J. Chem. Phys.* **1993**, *98*, 8718.

(27) (a) Dunning, T. H., Jr. *J. Chem. Phys.* **1989**, *90*, 1007. (b) Kendall, R. A.; Dunning, T. H., Jr.; Harrison, R. J. *J. Chem. Phys.* **1992**, *96*, 6796. (c) Woon, D. E.; Dunning, T. H., Jr. *J. Chem. Phys.* **1993**, *98*, 1358. (d) Dunning, T. H., Jr.; Wilson, A. K.; Peterson, K. A. *J. Chem. Phys.* **2001**, *114*, 9244.

(28) Dunham, J. L. *Phys. Rev.* **1932**, *41*, 721.

(29) Bauschlicher, C. W., Jr.; Ricca, A. *J. Phys. Chem. A* **1998**, *102*, 4722.

(30) Goddard, W. A., III.; Dunning, T. H., Jr.; Hunt, W. J.; Hay, P. J. *Acc. Chem. Res.* **1973**, *6*, 368.

(31) Yang, X.; Boggs, J. E. *J. Chem. Phys.* **2005**, *122*, 194307.

(32) Baluja, K. L.; Tossell, J. A. *J. Phys. B. At. Mol. Opt. Phys.* **2003**, *36*, 19.

(33) Hildenbrand, D. L. *J. Phys. Chem.* **1973**, *77*, 897.

(34) Fisher, E. R.; Kickel, B. L.; Armentrout, P. B. *J. Chem. Phys.* **1992**, *97*, 4859.

(35) Cheung, Y.-S.; Chen, Y.-J.; Ng, C. Y.; Chiu, S.-W.; Li, W.-K. *J. Am. Chem. Soc.* **1995**, *117*, 9725.

(36) Irikura, K. K. *J. Chem. Phys.* **1995**, *102*, 5357.

(37) Miller, T. M.; Arnold, S. T.; Viggiano, A. A. *Int. J. Mass. Spectrom.* **2003**, *227*, 413.

(38) Grant, D. J.; Matus, M. H.; Switzer, J. R.; Dixon, D. A.; Francisco, J. S.; Christie, K. O. *J. Phys. Chem. A* **2008**, *112*, 3145.

(39) Hassanzadeh, P.; Andrews, L. *J. Phys. Chem.* **1992**, *96*, 79.

(40) Carrington, A.; Currie, G. N.; Miller, T. A.; Levy, D. H. *J. Chem. Phys.* **1969**, *50*, 2726.

(41) Amano, T.; Hirota, E. *J. Mol. Spectrosc.* **1973**, *45*, 417.

(42) Endo, Y.; Saito, S.; Hirota, E. *J. Mol. Spectrosc.* **1982**, *92*, 443.

(43) Byfleet, C. R.; Carrington, A.; Russell, D. K. *Mol. Phys.* **1971**, *20*, 271.

(44) Peterson, K. A.; Woods, R. C. *J. Chem. Phys.* **1990**, *92*, 7412.

(45) Polak, M. L.; Gilles, M. K.; Lineberger, W. C. *J. Chem. Phys.* **1992**, *96*, 7191.

(46) Note that SF has other bound states with recoupled pair bonds. For example, the first $^2\Sigma^-$ state uses the same configuration diagram shown in Figure 4, but the unpaired electrons are coupled as a doublet rather than a quartet. The $^2\Sigma^-$ state is only weakly bound, by about 5 kcal/mol (see ref 31).

(47) The bond energy of SF($^2\Pi$) is smaller because the triplet coupling between the sulfur $3p_x$ and $3p_y$ electrons is disrupted when the SF bond is formed, resulting in a loss of exchange energy. This is well known in other species, such as the NH_n series. For a more detailed discussion, see ref 69d.

(48) Endo, Y.; Saito, S.; Hirota, E.; Chikaraishi, T. *J. Mol. Spectrosc.* **1979**, *77*, 222.

(49) Johnson, D. R.; Powell, F. X. *Science* **1969**, *164*, 950.

(50) Kirchhoff, W. H.; Johnson, D. R.; Powell, F. X. *J. Mol. Spectrosc.* **1973**, *48*, 157.

(51) (a) Liu, Y.-J.; Huang, M.-B.; Zhou, X.; Yu, S. *Chem. Phys. Lett.* **2001**, *345*, 505. (b) Czernek, J.; Živný, O. *Chem. Phys.* **2008**, *344*, 142.

(52) Yu, H.; Goddard, J. D.; Clouthier, D. J. *Chem. Phys. Lett.* **1991**, *178*, 341.

(53) Hay, P. J. *J. Am. Chem. Soc.* **1977**, *99*, 1003.

(54) Baird, N. C.; Kuhn, M.; Lauriston, T. M. *Can. J. Chem.* **1989**, *67*, 1952.

(55) Colussi, A. J.; Morton, J. R.; Preston, K. F.; Fessenden, R. W. *J. Chem. Phys.* **1974**, *61*, 1247.

(56) Tolles, W. M.; Gwinn, W. D. *J. Chem. Phys.* **1962**, *36*, 1119.

(57) Dodd, R. E.; Woodward, L. A.; Roberts, H. L. *Trans. Faraday Soc.* **1956**, *52*, 1052.

(58) Cotton, F. A.; George, J. W.; Waugh, J. S. *J. Chem. Phys.* **1958**, *28*, 994.

(59) Muetterties, E. L.; Phillips, W. D. *J. Am. Chem. Soc.* **1959**, *81*, 1084.

(60) Morton, J. R.; Preston, K. F. *Chem. Phys. Lett.* **1973**, *18*, 98.

(61) Fessenden, R. W.; Schuler, R. H. *J. Chem. Phys.* **1966**, *45*, 1845.

(62) Brockway, L. O.; Pauling, L. *Proc. Natl. Acad. Sci. U.S.A.* **1933**, *19*, 68.

(63) Ewing, V. C.; Sutton, L. E. *Trans. Faraday Soc.* **1963**, *59*, 1241.

(64) Kiang, T.; Estler, R. C.; Zare, R. N. *J. Chem. Phys.* **1979**, *70*, 5925.

(65) Babcock, L. M.; Streit, G. E. *J. Chem. Phys.* **1981**, *74*, 5700.

(66) Tsang, W.; Herron, J. T. *J. Chem. Phys.* **1992**, *96*, 4272.

(67) The larger spatial separation between the lobe orbitals in C compared with S is reflected in their respective overlaps, 0.73 in C and 0.90 in S. Compare the lobe orbitals in Figure 3a of ref 30 for C with those for S in Figure 3b of the present work.

(68) Kalemos, A.; Dunning, T. H., Jr. Private communication.

(69) (a) Blint, R. J.; Goddard, W. A., III. *Chem. Phys.* **1974**, *3*, 297. (b) Goddard, W. A., III.; Blint, R. J. *Chem. Phys. Lett.* **1972**, *14*, 616. (c) Hay, P. J.; Hunt, W. J.; Goddard, W. A., III. *J. Am. Chem. Soc.* **1972**, *94*, 8293. (d) Goddard, W. A., III.; Harding, L. B. *Annu. Rev. Phys. Chem.* **1978**, *29*, 363.

(70) (a) Livingston, H. K.; Sullivan, J. W.; Musher, J. I. *J. Polym. Soc. C* **1968**, *22*, 195. (b) Musher, J. I. *J. Am. Chem. Soc.* **1972**, *94*, 1370. (c) Musher, J. I. *Ann. N.Y. Acad. Sci.* **1972**, *192*, 52. (d) Koutecký, V. B.; Musher, J. I. *Theor. Chim. Acta* **1974**, *33*, 227.

(71) Woon, D. E.; Dunning, T. H., Jr. *Mol. Phys.* In press. DOI: 10.1080/00268970802712431.

JP901949B